2011 American Control Conference
on O'Farrell Street, San Francisco, CA, USA
June 29 - July 01, 2011

A new algorithm for frequency estimation and disturbance cancellation inspired from induction machine theory

Scott Pigg, *Grad. Student Member, IEEE,* and Marc Bodson, *Fellow, IEEE*

***Abstract*— The paper presents a new frequency estimation algorithm based on the model of a two-phase induction motor. Averaging theory is used to show that, for a small adaptation gain and positive initial conditions, the frequency estimator is globally stable. Local exponential convergence is obtained near the nominal frequency. Combined with a gradient-based adaptive algorithm for disturbance rejection, the frequency estimator rejects sinusoidal disturbances of unknown frequencies. Averaging theory is used to show global convergence of the combined algorithm. Active noise control experiments validate the results of the analysis, and show that the algorithm successfully rejects disturbances of unknown frequency, as well as with abrupt and slow frequency variations.**

I. Introduction

The need to reject a sinusoidal disturbance of unknown frequency is a problem frequently encountered in practice. In tape systems, reel eccentricities cause tension ripples that are mostly sinusoidal disturbances whose frequencies vary with tape position [12]. Similar disturbances are introduced by track eccentricities in CD players [2]. [6] deals with the reduction of low frequency optical jitter with an unknown frequency. In helicopters, sinusoidal vibrations with time-varying frequency occur due to the interaction of each blade tip with the air vortex created by the preceding blade [5]. Oftentimes, the frequency of the disturbance cannot be measured directly and may vary significantly with time.

A common technique for dealing with disturbances of unknown frequency is to first obtain an estimate of the unknown frequency, and then use this estimate in a disturbance cancellation algorithm for known frequency [1][11]. Thus, estimating the frequency of an unknown sinusoid has received much attention in the literature. While interesting solutions exist for frequency determination with batch processing of data, control applications typically require that one obtains an estimate that can be updated continuously and tracks time-variations. In [11], a phase-locked loop frequency estimate, derived from the magnitude/phase-locked loop (MPLL) estimator of [10], was used with a gradient-based disturbance cancelation algorithm. Active noise control experiments demonstrated the effectiveness of this approach. However, the stability of the MPLL algorithm required that the initial frequency estimate be sufficiently close to the true frequency [4].

The main objective of this paper is to show that a new type of frequency estimator can be obtained from models of AC (alternating current) electric machines. Specifically, induction machines are robust devices whose mechanical speed track the angular frequency of the electric currents applied to their windings. An induction motor model can therefore form the basis of a frequency estimator where the rotor speed is the estimate of the frequency. In practice, induction machines are asynchronous, meaning that the speed is slower than the electrical frequency, due to load and friction. However, when a no-load condition is simulated, global convergence of the frequency estimator can be obtained. The induction motor frequency estimation (IMFE) algorithm can also be combined with a disturbance cancellation algorithm to reject disturbances of unknown frequency. The approach was tested successfully in active noise control experiments using the disturbance cancelation algorithm of [11]. The need for an *a priori* estimate of the frequency was found to be relaxed with a negligible increase in computational complexity. Of significant interest is the fact that AC electric machines provide inspiration for a new type of frequency estimator, whose full advantages may yet to be discovered.

Electrical and Computer Engineering, University of Utah, 50 S Central Campus Dr Rm 3280, Salt Lake City, UT 84112, U.S.A.

This material is based upon work supported in part by Sandia National Laboratories.

II. Induction motor frequency estimation algorithm

A. Model of a two-phase induction motor

The model of a two-phase induction motor with one pole pair and current command is given by the equations

$$\begin{aligned} \frac{d\psi_{RA}}{dt} &= -\frac{1}{T_R}\psi_{RA} + \frac{M}{T_R} i_{SA} - \omega\psi_{RB} \\ \frac{d\psi_{RB}}{dt} &= -\frac{1}{T_R}\psi_{RB} + \frac{M}{T_R} i_{SB} + \omega\psi_{RA} \\ \frac{d\omega}{dt} &= \frac{M}{JL_R}\left(i_{SB}\ \psi_{RA} - i_{SA}\ \psi_{RB}\right) \end{aligned} \tag{1}$$

where ψ_{RA} and ψ_{RB} are the total rotor flux linkages along phases A and B, i_{SA} and i_{SB} are the currents in the phase windings A and B, T_R is the rotor time constant, M is the mutual inductance between the stator and the rotor, ω is the mechanical speed of the rotor, J is the inertia of the rotor, and L_R is the rotor self-inductance. The model assumes that there is no load or friction torque.

The currents in the stator windings are assumed to be of the form

$$\begin{pmatrix} i_{SA} \\ i_{SB} \end{pmatrix} = I_m \begin{pmatrix} \cos(\omega_e t) \\ \sin(\omega_e t) \end{pmatrix} \tag{2}$$

where ω_e is the (angular) electrical frequency of the sinusoidal currents. The difference between the two frequencies, $S = \omega_e - \omega$, is an important quantity known as the *slip frequency*. The torque generated by the motor is a nonlinear

function of the slip frequency, but is approximately linear for small slip. Thus, for small S, induction motor theory predicts that

$$\frac{d\omega}{dt} \simeq k(\omega_e - \omega) \tag{3}$$

for some constant k. Therefore, the rotor speed converges to the electrical frequency with the desirable dynamics of a first-order system. For large slip, the torque is reduced, but remains of the same sign, so that global convergence of ω to ω_e is ensured.

B. IMFE algorithm

Consider now the task of estimating the frequency ω_1^* of a sinusoidal signal

$$y(t) = m^* \cos(\alpha_1^*(t)) \tag{4}$$

where $\alpha_1^*(t) = \omega_1^* t$. We propose to solve this problem by implementing an induction motor model with ω becoming the estimate ω_1 of ω_1^*. Thus, the algorithm will be given by

$$\begin{aligned} \dot{x}_{1F}(t) &= -a_1 x_{1F} + a_1 x_1 - \omega_1 x_{2F} && (5) \\ \dot{x}_{2F}(t) &= -a_1 x_{2F} + a_1 x_2 + \omega_1 x_{1F} && (6) \end{aligned}$$

and

$$\dot{\omega}_1 = g_\omega \left(x_2(t) x_{1F}(t) - x_1(t) x_{2F}(t) \right) \tag{7}$$

where a_1 and g_ω are positive constants. Note that x_1 can be defined as Mi_{SA} so that the two constants in (5)-(6) can be assumed to be equal.

The signal x_1 is simply

$$x_1(t) = y(t) \tag{8}$$

but a difficulty is that the signal x_2 associated with the second winding is not available. The situation has a parallel in induction machines operated on residential single-phase supplies, where single-phase induction motors are two-phase motors with the second winding connected in series to a capacitor, and then in parallel with the first winding. The capacitor is selected so that the current in the second winding is approximately 90° out of phase with the first winding.

In the context of a numerical frequency estimator, the limitations of a physical implementation can be avoided, and other means of shifting the phase by 90° can be used. For example, a possible choice is the filter

$$H_1(s) = \frac{\omega_1 - s}{s + \omega_1} \tag{9}$$

which has a gain of 1 and a phase lead of 90° at frequency ω_1. An approximation of the second winding current is the signal $x_2(t)$ defined through

$$x_2(t) = H_1(s) \left[x_1(t) \right] \tag{10}$$

where the notation $H_1(s)[\cdot]$ represents the time domain output of the system with transfer function $H_1(s)$. (10) can be implemented as

$$\begin{aligned} \dot{x}_3 &= -\omega_1 x_3 + \omega_1 x_1 \\ x_2 &= 2x_3 - x_1 && (11) \end{aligned}$$

The overall frequency estimator is defined by (5),(6), (7), and (11). The algorithm is quite different from other frequency estimation aglorithms, such as [7], [8].

C. Stability analysis of the IMFE algorithm using averaging

The system can be fitted in the averaging theory for mixed time scales systems [9], where the frequency estimate (7) varies slowly, and the signals (8), (10) and (5)-(6) vary at a faster or mixed time scale. In finding the averaged system, the frequency estimate is held constant, and the responses of the fast variables are approximated by their steady-state responses. Then, x_1 and x_3 become

$$\begin{aligned} x_1 &= m^* \cos(\alpha_1^*) && (12) \\ x_3 &= \frac{m^*}{\omega_1^2 + \omega_1^{*2}} \left(\omega_1^2 \cos(\alpha_1^*) + \omega_1 \omega_1^* \sin(\alpha_1^*) \right) && (13) \end{aligned}$$

To find the steady-state values of the filtered signals (5)-(6), rewrite the equations as

$$\begin{aligned} x_{1F} &= H_2(s) \left[x_1 \right] - H_3(s) \left[2x_3 - x_1 \right] && (14) \\ x_{2F} &= H_2(s) \left[2x_3 - x_1 \right] + H_3(s) \left[x_1 \right] && (15) \end{aligned}$$

where

$$\begin{aligned} H_2(s) &= \frac{a_1 (s + a_1)}{(s + a_1)^2 + \omega_1^2} && (16) \\ H_3(s) &= \frac{a_1 \omega_1}{(s + a_1)^2 + \omega_1^2} && (17) \end{aligned}$$

Next, define the real and imaginary parts of the frequency responses of the three filters (9), (16), and (17) with

$$\begin{aligned} H_1(j\omega_1^*) &= H_{R1} + jH_{I1} && (18) \\ H_2(j\omega_1^*) &= H_{R2} + jH_{I2} && (19) \\ H_3(j\omega_1^*) &= H_{R3} + jH_{I3} && (20) \end{aligned}$$

The steady-state values of (14)-(15) are then given by

$$\begin{aligned} x_{1F} &= m^* w_1^{*T}(t) \left(\begin{pmatrix} H_{R2} \\ H_{I2} \end{pmatrix} - \begin{pmatrix} H_{R3} & -H_{I3} \\ H_{I3} & H_{R3} \end{pmatrix} \times \begin{pmatrix} H_{R1} \\ H_{I1} \end{pmatrix} \right) && (21) \\ x_{2F} &= m^* w_1^{*T}(t) \left(\begin{pmatrix} H_{R2} & -H_{I2} \\ H_{I2} & H_{R2} \end{pmatrix} \begin{pmatrix} H_{R1} \\ H_{I1} \end{pmatrix} + \begin{pmatrix} H_{R3} \\ H_{I3} \end{pmatrix} \right) && (22) \end{aligned}$$

where

$$w_1^*(t) = \begin{pmatrix} \cos(\alpha_1^*(t)) \\ -\sin(\alpha_1^*(t)) \end{pmatrix} \tag{23}$$

Given the steady-state values, the right side of the frequency estimator equation (7) can be averaged with

$$\begin{aligned} AVE\left[x_2 x_{1F} - x_1 x_{2F} \right] &= \frac{m^{*2}}{2} \left(2H_{I1} H_{I2} - H_{R3} \times \left(H_{R1}^2 + H_{I1}^2 + 1 \right) \right) && (24) \end{aligned}$$

Using (18), (19) and (20), the averaged system is given by

$$\dot{\omega}_1 = -g_\omega f_{av}(\omega_1) \tag{25}$$

with

$$f_{av}(\omega_1) = \frac{m^{*2}a_1\omega_1}{(\omega_1^2+\omega_1^{*2})}\frac{3\omega_1^{*2}+\omega_1^2+a_1^2}{\left(\omega_1^2-\omega_1^{*2}+a_1^2\right)^2+\left(2a_1\omega_1^*\right)^2} \times\left(\omega_1^2-\omega_1^{*2}\right) \quad (26)$$

To assess the stability of (25), note that $f_{av}(\omega_1)=0$ implies the existence of three real equilibrium points at $\omega_1=0$ and $\omega_1=\pm\omega_1^*$. Evaluating $\partial f_{av}/\partial\omega_1$ at the equilibrium points gives

$$\left.\frac{\partial f_{av}}{\partial\omega_1}\right|_{\omega_1=0} = g_\omega m^{*2}\frac{a_1\left(3\omega_1^{*2}+a_1^2\right)}{\left(\omega_1^{*2}+a_1^2\right)^2} \quad (27)$$

$$\left.\frac{\partial f_{av}}{\partial\omega_1}\right|_{\omega_1=\pm\omega_1^*} = -g_\omega m^{*2}\frac{1}{a_1} \quad (28)$$

The equilibrium point $\omega_1=0$ is repulsive, while $\omega_1=\pm\omega_1^*$ are both attractive. Thus, with a positive initial estimate $\omega_1(0)$, ω_1 will converge to ω_1^*. As $\omega_1\to\omega_1^*$ (25) becomes, approximately

$$\dot\omega_1 \simeq -\frac{g_\omega m^{*2}}{2a_1}\left(\omega_1-\omega_1^*\right) \quad (29)$$

so that convergence is exponential in the vicinity of ω_1^*. The exponential convergence around ω_1^* is comparable to the linear convergence of the induction motor for small slip. The quadrature filter (9) is the source of the two additional equilibrium points, which are not useful, but do not cause any problem either.

D. Discrete-time implementation

The implementation of the estimator on a microprocessor requires the derivation of a set of difference equations that can be used to recursively update the system states. The algorithm is implemented by deriving an equivalent discrete-time algorithm. The input of the estimator is the discrete-time signal

$$x_1(k)=y(k) \quad (30)$$

Let $\Omega_1(k)$ be the estimate of the discrete-time frequency $\Omega_1^*=\omega_1^*T_S$, where T_S is the sampling period. Define the auxiliary signal

$$r(k)=\cos(\Omega_1(k))/\left(1+\sin(\Omega_1(k))\right) \quad (31)$$

The discrete-time algorithm is given by

$$x_3(k) = r(k)x_3(k-1)+x_1(k-1) \quad (32)$$

$$x_{1F}(k+1) = a_{d1}x_{1F}(k)+\left(1-a_{d1}\right)x_1(k) -\sin\left(\Omega_1(k)\right)x_{2F}(k) \quad (33)$$

$$x_{2F}(k+1) = a_{d1}x_{2F}(k)+\left(1-a_{d1}\right)x_2(k) +\sin\left(\Omega_1(k)\right)x_{1F}(k) \quad (34)$$

where $a_{d1}=1-a_1T_S$ and

$$x_2(k+1)=\left(1-r(k)^2\right)x_3(k)-r(k)x_1(k) \quad (35)$$

The frequency update is given by

$$\Omega_1(k+1)=\Omega_1(k)+g_df_d \quad (36)$$

with

$$f_d = x_2(k)x_{1F}(k+1)-x_1(k)x_{2F}(k+1)$$

$$g_d = g_\omega T_S^2 \quad (37)$$

III. Application of the IMFE algorithm in sinusoidal disturbance cancellation

A. Gradient based disturbance cancellation

The IMFE can be combined with a gradient-based disturbance cancellation algorithm to reject sinusoidal disturbances of unknown frequency. Given the system $P(s)$, consider the output

$$y(t)=P(s)\left[u(t)+d(t)\right] \quad (38)$$

The goal is to find an appropriate input $u(t)$ such that $y(t)$ is minimized. Express the disturbance as

$$d(t)=w_1^{*T}(t)\pi,\quad \pi=\begin{pmatrix} d_c\\ d_s\end{pmatrix} \quad (39)$$

d_c and d_s are unknown parameters. w_1^* is given by (23) where $\alpha_1^*(t)=\omega_1^*t$ and ω_1^* is the frequency of the disturbance.

The control signal is chosen to be

$$u(t)=w_1^T(t)\theta,\quad \theta=\begin{pmatrix}\theta_c\\ \theta_s\end{pmatrix} \quad (40)$$

where

$$w_1(t)=\begin{pmatrix}\cos(\alpha_1(t))\\ -\sin(\alpha_1(t))\end{pmatrix} \quad (41)$$

and the phase

$$\alpha_1(t)=\int_0^t\omega_1 d\tau \quad (42)$$

where ω_1 is an estimate of the frequency of the disturbance.

The so-called inverse-G algorithm [11] is a gradient-based algorithm that updates θ using

$$\dot\theta(t)=-gG^Tw_1(t)y(t). \quad (43)$$

where $g>0$ is an adaptation gain,

$$G=\begin{pmatrix}P_R & -P_I\\ P_I & P_R\end{pmatrix} \quad (44)$$

and P_R, P_I are the real and imaginary parts of the frequency response at the estimated frequency, *i.e.,* $P(j\omega_1)=P_R+jP_I$.

The disturbance cancellation algorithm can be combined with the IMFE algorithm by using the frequency estimate ω_1 of the IMFE in the reconstruction of the angle α_1. One difficulty is that the control signal produces an output that interferes with the frequency estimator. The problem can be avoided by using in the IMFE a modified signal

$$x_1=y(t)-P(s)[u(t)]=P(s)[d(t)] \quad (45)$$

so that the signal used by the IMFE is the same as if the control input was zero. Alternatively, the signal x_1 can be replaced by the simpler expression

$$x_1=y(t)-w_1^TG\theta \quad (46)$$

which corresponds to a steady-state approximation with slowly varying parameter θ. The implementation is especially useful if the plant is difficult to model with a finite-order transfer function (due to delays, resonances,...). A frequency response can often be obtained accurately in practice, even when a good finite-order fit cannot be obtained. Fig. 1, shows a diagram of the overall closed-loop system (with $y_u = w_1^T \hat{G}\theta$ and $\hat{G}$ is an estimate of G).

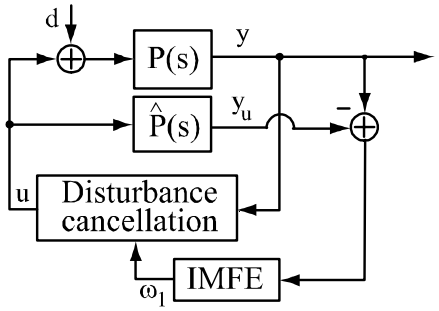

Fig. 1. Diagram of indirect disturbance cancelation with IMFE frequency estimation.

B. Averaging analysis of the overall adaptive system

The states of the closed-loop system can be divided into two sets, a set of slow variables and a set of fast variables. Assuming that the adaptive gains g and g_ω are small, the slow variables are the control parameter vector and the frequency estimate, described by

$$\begin{aligned} \dot{\theta} &= -gG^T w_1 y \quad (47) \\ \dot{\omega}_1 &= g_\omega \left(x_2 x_{1F} - x_1 x_{2F}\right) \quad (48) \end{aligned}$$

With x_P denoting the internal states of $P(s)$, the fast variables consist of the plant states

$$\begin{aligned} \dot{x}_P &= Ax_P + B\left(w_1^{*T}\pi - w_1^T\theta\right) \\ y &= Cx_P \end{aligned} \quad (49)$$

as well as the IMFE dynamics

$$\begin{aligned} \dot{x}_3 &= -\omega_1 x_3 + \omega_1 x_1 \\ \dot{x}_{1F} &= -a_1 x_{1F} + a x_1 - \omega_1 x_{2F} \\ \dot{x}_{2F} &= -a_1 x_{2F} + a x_2 + \omega_1 x_{1F} \\ x_1 &= y - w_1^T G\theta \\ x_2 &= 2x_3 - x_1 \end{aligned} \quad (50)$$

Using the technique of [3], the angle α_1 can also be treated as a slow variable.

In finding the averaged system corresponding to (47)-(50), the responses of the fast variables are taken as the steady-state responses, and the dynamics of the slow variables are averaged over time. Thus, the frequency estimate and the control vector θ are assumed to be constant in calculating the responses of the fast variables. The averaged system for the IMFE is the same as was derived earlier because, for $P(s) = \hat{P}(s)$, in steady-state

$$x_1 = y_{ss} + P(s)[d(t)] - w_1^T G\theta = P(s)[d(t)] \quad (51)$$

The stability result from Sec. II.C applies: for g_ω sufficiently small, the frequency estimate ω_1 converges to the disturbance frequency ω_1^*. Close to the disturbance frequency, convergence is exponential.

For the disturbance cancellation component, the steady-state output of the plant can be written

$$y_{ss} = w_1^T G\left(\theta - \theta^*\right) \quad (52)$$

where

$$\theta^* = -\begin{pmatrix} \cos(\tilde{\alpha}) & \sin(\tilde{\alpha}) \\ -\sin(\tilde{\alpha}) & \cos(\tilde{\alpha}) \end{pmatrix}\pi \quad (53)$$

and $\tilde{\alpha} = \alpha_1 - \alpha_1^*$. The averaged dynamics of the control parameter update are given by

$$\dot{\theta}(t) = -\frac{g}{2}(P_R^2 + P_I^2)\left(\theta - \theta^*\right) \quad (54)$$

For $\omega_1 = \omega_1^*$, the control signal converges to

$$u(t) = -w_1^{*T}\pi \quad (55)$$

Thus, as the frequency error $\omega_1 \to \omega_1^*$, θ converges exponentially to a value θ^*such that the disturbance is exactly canceled. Note that the equilibrium θ^* is not unique, as it depends on the phase associated with the integration of the frequency estimate. However, this non-uniqueness simply produces a rotation of the control vector without the dangers normally associated with non-uniqueness and parameter drift.

C. Experimental results

The performance of the inverse-G/IMFE algorithm was examined through single-channel active noise control experiments. (47) was discretized using the Euler approximation so that

$$\theta(k) = \theta(k-1) - g_\theta G^T w_1(k-1)y(k). \quad (56)$$

where $g_\theta = gT_S$, and the IMFE was discretized as in Sec. II.D. The algorithm was coded in C and implemented in a dSPACE DS1104 digital signal processing board. A sampling frequency of $8\ kHz$ was used. A constant amplitude sinusoidal disturbance with frequency of $160\ Hz$ was generated by a loudspeaker, while the control signal was produced by another loudspeaker. A microphone was used to measure the cancellation error. The plant consists of the hardware and transmission in the environment from the control signal output to the error microphone input, including the propagation effects of the surrounding air. The experiments were conducted in a small room where many signal reflections were present. In all experiments, the following parameters were used: $a_{d1} = 0.6875$, $g_{d1} = 31.25 \times 10^{-6}$, $g_\theta = 0.001875$.

In the first experiment, the initial IMFE frequency was $f_1(0) = 130\ Hz$ for an initial frequency error of $50\ Hz$. After 2 seconds, the inverse-G and the IMFE were engaged simultaneously, and the algorithm was allowed to reach steady-state. After approximately 3.5 seconds, the frequency of the disturbance was increased by an additional $50\ Hz$. Fig. 2 shows the frequency estimate and Fig. 3 shows the measured output y. The figures show that the algorithm is

able to adjust for the change in frequency while maintaining significant rejection of the disturbance. The components of the control vector θ are shown in Fig. 4.

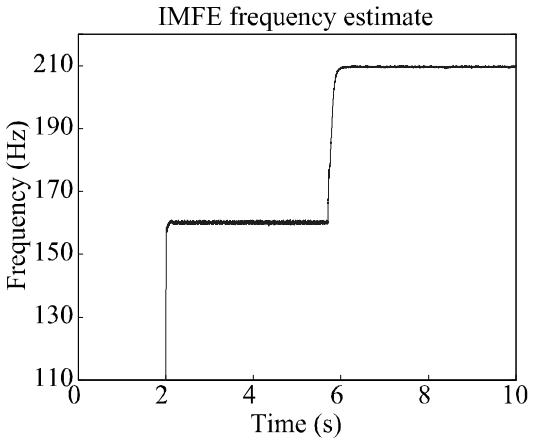

Fig. 2. IMFE frequency estimate.

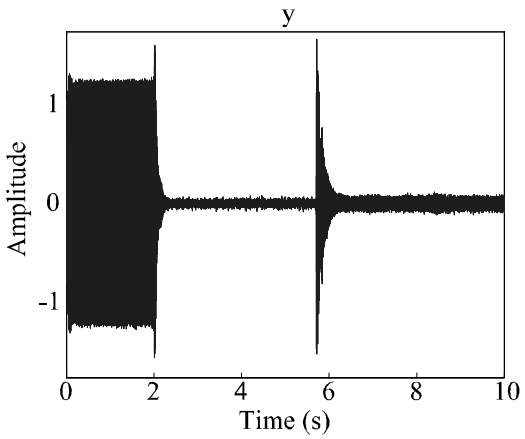

Fig. 3. Measured output with inverse-G disturbance cancelation and IMFE frequency estimation.

In the second experiment, the IMFE frequency estimator tracks a slowly varying disturbance frequency. After 2 seconds, the inverse-G and the IMFE were engaged simultaneously, and the algorithm was allowed to reach steady-state. Approximately 3 seconds later, the frequency of the disturbance was increased at a rate of 15 Hz per 10 seconds. In Fig. 5, the ability of the algorithm to track a slowly varying frequency is shown, and in Fig. 6, significant attenuation of the disturbance is seen despite the changing frequency. The components of the control vector θ are shown in Fig. 7.

In the next experiment, results using the inverse-G disturbance cancelation algorithm and a MPLL frequency estimator are shown for comparison (implementing the algorithm of [3]). The initial frequency estimate was set at $f_1(0) = 150\ Hz$, closer to the true value to insure convergence of the MPLL algorithm. After 2 seconds, the algorithm was engaged, resulting in significant attenuation of

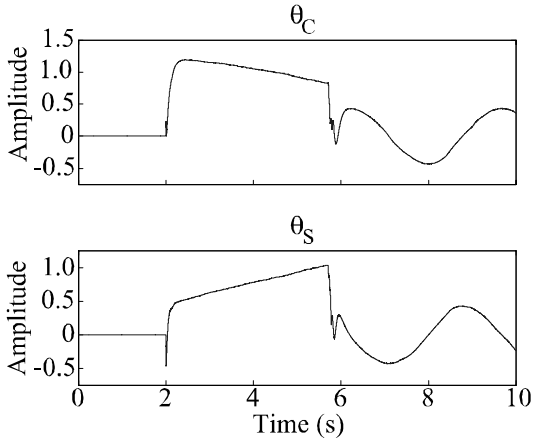

Fig. 4. θ with IMFE frequency estimation.

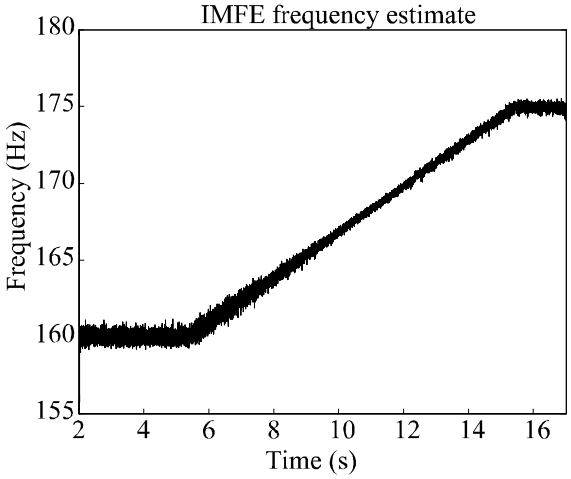

Fig. 5. IMFE frequency estimate tracking changes in the disturbance frequency.

the disturbance. After an additional 4 seconds, the frequency of the disturbance was increased by 50 Hz. Fig. 8 shows the MPLL frequency. The MPLL frequency estimator was not able to compensate for the change in frequency. Fig. 9 shows the measured output y, which exhibits good reduction under tracking conditions, but large errors otherwise.

IV. Conclusions

In this paper, a new frequency estimator was presented, derived from the model of a two phase induction motor. Averaging theory was used to show that global convergence (for positive initial conditions) of the frequency estimator was ensured, with local exponential stability around the nominal value. The IMFE was combined with a gradient-based disturbance cancellation algorithm for the rejection of sinusoidal disturbances of unknown frequency. Averaging theory was used to show that the resulting disturbance cancelation algorithm was also globally convergent, with an assumption of small gains. Active noise control experiments were used to demonstrate performance of the algorithm and

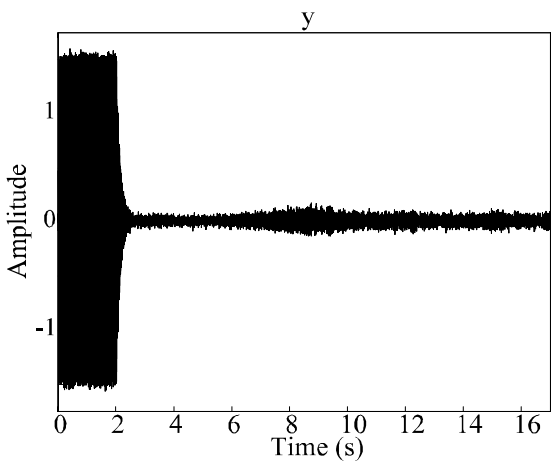

Fig. 6. Measured output with inverse-G disturbance cancelation and IMFE frequency tracking.

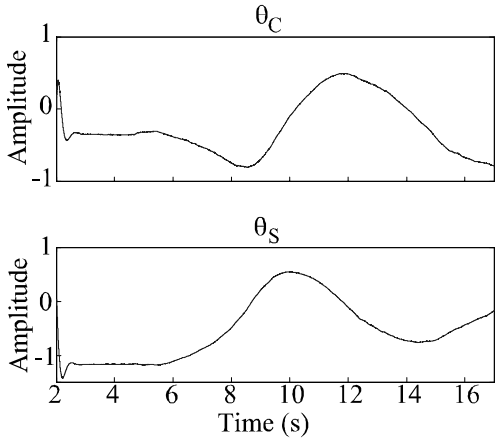

Fig. 7. θ with IMFE frequency tracking.

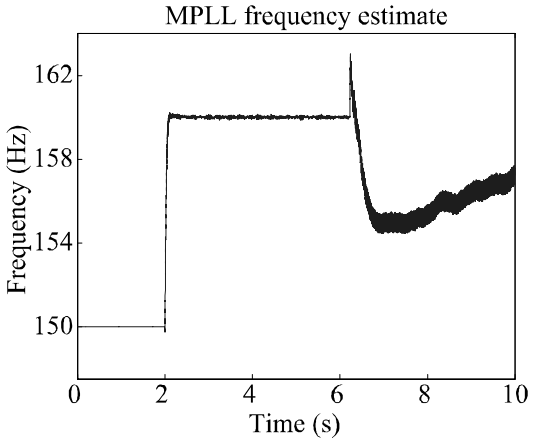

Fig. 8. MPLL frequency estimate.

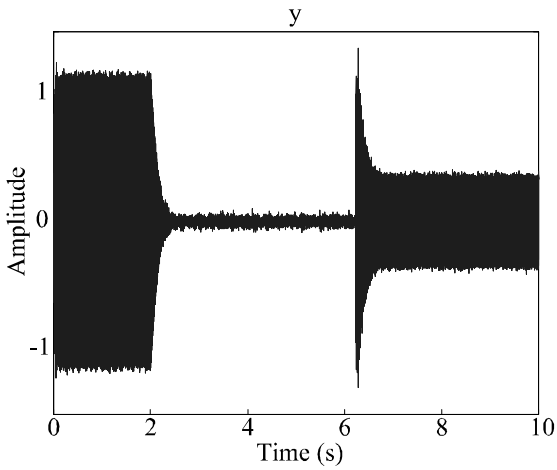

Fig. 9. Measured output with inverse-G disturbance cancelation and MPLL frequency estimation.

to verify the results of the analysis. Further research is needed to extend the algorithm for the rejection of disturbances containg multiple sinusoidal components, and cases where the plant frequency response is unknown and time-varying.

REFERENCES

[1] M. Bodson & S. Douglas, "Adaptive Algorithms for the Rejection of Sinusoidal Disturbances with Unknown Frequency," *Automatica*, vol. 33, no. 12, pp. 2213-2221, 1997.

[2] H. G .M. Dötsch, H. T. Smakman, P. M. J. Van den Hof, & M. Steinbuch, "Adaptive Repetitive Control of a Compact Disc Mechanism," *Proc. of the Conference on Decision and Control*, New Orleans, LA, pp. 1720-1725, 1995.

[3] X. Guo & M. Bodson, "Frequency Estimation and Tracking of Multiple Sinusoidal Components," *Proc. of the Conference on Decision and Control*, Maui, HI, pp. 5360-5365, 2003.

[4] X. Guo & M. Bodson, "Analysis and Implementation of an Adaptive Algorithm for the Rejection of Multiple Sinusoidal Disturbances," *IEEE Trans. on Control Systems Technology*, vol. 17, no. 1, pp. 40-50, 2009.

[5] S. Hall & N. Wereley, "Performance of higher harmonic control algorithms for helicopter vibration reduction," *J. Guidance Contr. Dynam.*, vol. 116, no. 4, pp. 793–797, 1993.

[6] M. A. McEver, D. G. Cole, & R. L. Clark, "Adaptive Feedback Control of Optical Jitter Using Q-parameterization," *Opt. Eng.*, vol. 43, no. 4, pp. 904-910, 2004.

[7] R. Morino & P. Tomei, "Global estimation of n unknown frequencies," *IEEE Trans. on Automatic Control*, vol. 47, no. 8, pp. 1324—1328, 2002.

[8] G. O.-Pulido, B. C.-Toledo, & A. Loukianov, "A globally convergent estimator for n—frequencies," *IEEE Trans. on Automatic Control*, vol. 47, no. 5, pp. 857—863, 2002.

[9] S. Sastry & M. Bodson, *Adaptive Control: Stability, Convergence, and Robustness*, New Jersey, Prentice Hall, Englewood Cliffs, 1989.

[10] B. Wu & M. Bodson, "A Magnitude/Phase-locked Loop Approach to Parameter Estimation of Periodic Signals," *IEEE Trans. on Automatic Control*, vol. 48, no. 4, pp. 612-618, 2003.

[11] B. Wu & M. Bodson, "Multi-Channel Active Noise Control for Periodic Sources – Indirect Approach," *Automatica*, vol 40, no. 2, pp. 203-212, 2004.

[12] H. Zhong, V. Kulkarni, & L. Pao, "Adaptive Control for Rejecting Disturbances with Time-varying Frequencies in Tape Systems," *Proc. of the American Control Conference*, Portland, OR, pp. 533-538, 2005.